Millimeter Wave Analog Beamforming Codebooks Robust to Self-Interference

Ian P. Roberts*, Hardik B. Jain†, Sriram Vishwanath†, and Jeffrey G. Andrews*
*University of Texas at Austin, Austin, TX, USA.
†GenXComm, Inc., Austin, TX, USA.

***Abstract*—This paper develops a novel methodology for designing analog beamforming codebooks for full-duplex millimeter wave (mmWave) transceivers, the first such codebooks to the best of our knowledge. Our design reduces the self-interference coupled by transmit-receive beam pairs and simultaneously delivers high beamforming gain over desired coverage regions, allowing mmWave full-duplex systems to support beam alignment while minimizing self-interference. To do so, our methodology allows some variability in beamforming gain to strategically shape beams that reject self-interference while still having substantial gain. We present an algorithm for approximately solving our codebook design problem while accounting for the non-convexity posed by digitally-controlled phase shifters and attenuators. Numerical results suggest that our design can outperform or nearly match existing codebooks in sum spectral efficiency across a wide range of self-interference power levels. Results show that our design offers an extra 20–50 dB of robustness to self-interference, depending on hardware constraints.**

I. Introduction

Codebook-based analog beamforming is a critical component of modern millimeter wave (mmWave) systems [1]. Rather than measure the complete over-the-air channel and subsequently configure analog beamformers, current mmWave systems instead rely on beam alignment procedures to more quickly identify promising transmit and receive beamforming directions, typically via exploration of a codebook of candidate analog beams [1], [2]. This offers a simple and robust way to configure dozens of phase shifters and attenuators without extensive channel knowledge *a priori*.

Designing analog beamforming codebooks that span a desired coverage region is relatively straightforward for conventional half-duplex mmWave systems [2]. Conjugate beamforming (i.e., matched filter beamforming), for example, is a simple way to construct a set of beams that serve desired directions and only requires phase shifters, not attenuators [3]. Other designs leverage attenuators to shape beams that exhibit wider main lobes and suppress side lobes, for example, which can reduce beam misalignment losses and inter-user interference.

Equipping mmWave systems with full-duplex capability is an attractive proposition at not only the physical layer but also as a deployment solution through integrated access and backhaul (IAB) [4]. To enable mmWave full-duplex, recent work [5]–[14] has explored beamforming-based self-interference mitigation in various contexts. Some designs [5]–[11] have neglected codebook-based analog beamforming, assuming the ability to fine-tune each phase shifter dynamically, and do not account for *digitally*-controlled phase shifters. Most designs have assumed a lack of amplitude control, even though it is not uncommon to have both phase shifters and attenuators in practical analog beamforming networks. In addition, existing solutions [5]–[12] have assumed transmit and receive channel knowledge along with that of the self-interference channel to configure precoding and combining—meaning they neglect beam alignment and rely on highly dynamic updates as the transmit and receive channels change.

Like half-duplex mmWave systems, one with full-duplex capability will presumably conduct codebook-based beam alignment on its transmit link *and* receive link, meaning it will juggle a transmit beam and receive beam concurrently, which couple together via the self-interference channel. Off-the-shelf analog beamforming codebooks that were designed for half-duplex settings may be undesirable in full-duplex settings since they do not necessarily offer robustness to self-interference [4]. Instead, we design analog beamforming codebooks for full-duplex that reliably deliver high beamforming gain to users and simultaneously reject self-interference regardless of which transmit and receive beams are used. Given such a codebook, standard beam alignment procedures that are self-interference agnostic can be utilized in a full-duplex system. This is a desirable practical outcome from our approach.

Among existing literature, we are not aware of any work on the design of analog beamforming *codebooks* for mmWave full-duplex. Our main contribution is a methodology for designing transmit and receive analog beamforming codebooks that reduces the average self-interference coupled between transmit-receive beam pairs while also guaranteeing the beamforming gain they provide. We present an algorithm for approximately solving for our design that addresses the non-convexity posed by digitally-controlled phase shifters and attenuators. Results indicate that our design offers 20–50 dB of added robustness to self-interference by strategically shaping beams with gain comparable to conventional codebooks.

As a result, codebooks designed with our approach could improve existing mmWave full-duplex work [11]–[14] that accounts for codebook-based analog beamforming. Hybrid digital/analog beamforming full-duplex systems could leverage our codebooks by weakening the *effective* self-interference channel post beam alignment. Perhaps most excitingly, a mmWave system employing our codebook design can in principle execute beam alignment and then seamlessly operate in a full-duplex fashion, thanks to codebooks whose beams offer inherent robustness to self-interference.

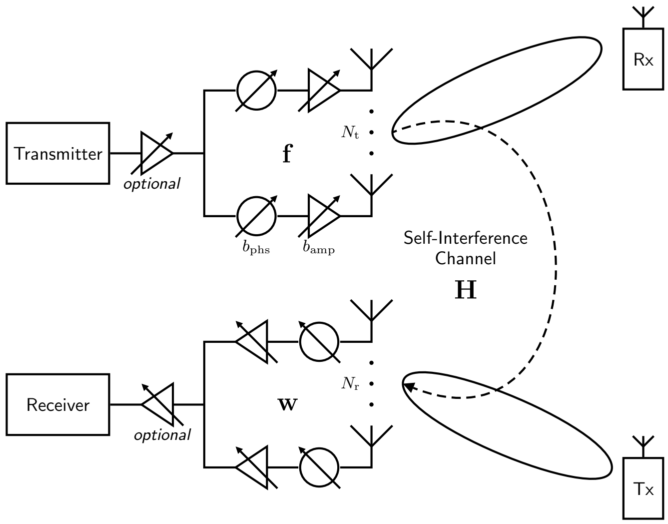

Fig. 1. A full-duplex mmWave transceiver with analog beamforming serving an uplink user with its receive beam and downlink user with its transmit beam.

II. System Model

In this work, we consider an in-band full-duplex mmWave transceiver that employs separate, independently controlled arrays for transmission and reception, as illustrated in Fig. 1. Let N_{t} and N_{r} be the number of transmit and receive antennas, respectively, at the arrays of the full-duplex transceiver. We denote as $\mathbf{a}_{\mathrm{tx}}(\vartheta) \in \mathbb{C}^{N_{\mathrm{t}} \times 1}$ and $\mathbf{a}_{\mathrm{rx}}(\vartheta) \in \mathbb{C}^{N_{\mathrm{r}} \times 1}$ the transmit and receive array response vectors, respectively, in the direction ϑ. We use the convention where $\|\mathbf{a}_{\mathrm{tx}}(\vartheta)\|_2^2 = N_{\mathrm{t}}$ and $\|\mathbf{a}_{\mathrm{rx}}(\vartheta)\|_2^2 = N_{\mathrm{r}}$.

We consider an analog-only beamforming system, though the codebook design herein could also be used by hybrid beamforming systems. Let $\mathbf{f} \in \mathbb{C}^{N_{\mathrm{t}} \times 1}$ be the analog precoding vector used at the transmitter and $\mathbf{w} \in \mathbb{C}^{N_{\mathrm{r}} \times 1}$ be the analog combining vector used at the receiver. We consider the practical case where the phase shifters and attenuators of the analog beamforming networks are digitally-controlled with b_{phs} and b_{amp} bits of resolution, respectively. We assume the set of all $2^{b_{\mathrm{phs}}}$ possible phase shifter settings are uniformly distributed over the range $[0, 2\pi)$ radians. We enforce that each beamforming weight not exceed unit magnitude, understood by the fact that attenuators are used to implement amplitude control. We assume the set of all $2^{b_{\mathrm{amp}}}$ possible attenuator settings are (arbitrarily) distributed over the range $(0, 1]$; it is practical to have an attenuation step size of 0.25 or 0.5 dB per least significant bit (LSB). Capturing limited phase and amplitude control, let $\mathcal{F} \subset \mathbb{C}^{N_{\mathrm{t}} \times 1}$ and $\mathcal{W} \subset \mathbb{C}^{N_{\mathrm{r}} \times 1}$ be the sets of all possible beamforming vectors $\mathbf{f}$ and $\mathbf{w}$, respectively.

Since transmission and reception happen simultaneously and in-band, a self-interference channel $\mathbf{H} \in \mathbb{C}^{N_{\mathrm{r}} \times N_{\mathrm{t}}}$ manifests between the transmit and receive arrays of the full-duplex transceiver. It is difficult to reliably assume a characterization or model for $\mathbf{H}$ given a lack of measurements. As such, we do not present a design based on any assumption of $\mathbf{H}$ but will evaluate our design using a commonly used near-field model.

A transmitted symbol s from the full-duplex transceiver will be injected into the self-interference channel $\mathbf{H}$ by its transmit beam $\mathbf{f}$ and transmit power gain P, then subsequently combined by its receive beam $\mathbf{w}$. To abstract out the large-scale gain of the self-interference channel from its spatial characteristics, we impose $\mathbb{E}\left[\|\mathbf{H}\|_{\mathrm{F}}^2\right] = N_{\mathrm{t}} \cdot N_{\mathrm{r}}$ and let a scalar $G \geq 0$ handle proper scaling of $\mathbf{H}$ based on the isolation between the arrays (practically, $G \ll 1$). The received self-interference y can thus be written as

$$y = \sqrt{P} \cdot G \cdot \mathbf{w}^* \mathbf{H} \mathbf{f} s. \quad (1)$$

It can be readily seen that decreasing the large-scale gain G (increasing isolation) would reduce self-interference as well as strategically steering $\mathbf{f}$ and $\mathbf{w}$ according to the channel $\mathbf{H}$.

III. Analog Beamforming Codebook Design

While transmit beams $\mathbf{f}$ are *fundamentally* limited to come from $\mathcal{F}$ and likewise $\mathbf{w}$ from $\mathcal{W}$, engineers establish smaller codebooks $\bar{\mathcal{F}} \subset \mathcal{F}$ and $\bar{\mathcal{W}} \subset \mathcal{W}$ from which $\mathbf{f}$ and $\mathbf{w}$ will be drawn, respectively (e.g., via beam alignment). We refer to the sizes of these codebooks as $|\bar{\mathcal{F}}| = M_{\mathrm{tx}}$ and $|\bar{\mathcal{W}}| = M_{\mathrm{rx}}$, which are much smaller than their counterparts $\mathcal{F}$ and $\mathcal{W}$.

A transmit beam $\mathbf{f}$ and receive beam $\mathbf{w}$, chosen from some codebooks $\bar{\mathcal{F}}$ and $\bar{\mathcal{W}}$, couple together via the self-interference channel $\mathbf{H}$. Off-the-shelf codebooks for conventional half-duplex mmWave systems (e.g., conjugate beams, discrete Fourier transform (DFT) codebooks) do not necessarily offer much robustness to self-interference [4]. Since even small amounts of self-interference can prohibit full-duplex operation, we are motivated us to design codebooks $\bar{\mathcal{F}}$ and $\bar{\mathcal{W}}$ *with full-duplex in mind*, such that self-interference is better rejected across all transmit-receive beam pairs while maintaining high beamforming gain.

To justify the construction of these codebooks, we assume the self-interference channel $\mathbf{H}$—little of which is currently known—can be estimated accurately and is sufficiently static over long periods. We conduct our design under the assumption of perfect knowledge of $\mathbf{H}$ and reserve future work for addressing imperfect channel knowledge. Practically, we envision conducting thorough estimation of $\mathbf{H}$ and execution of our design during initial setup of the transceiver and performing updates to the estimate of $\mathbf{H}$ and to our design.

A. Quantifying our Codebook Design Criteria

It is critical that our analog beamforming codebook offer high beamforming gain across a desired coverage region to combat severe mmWave path loss . Let $\mathcal{A}_{\mathrm{tx}}$ be a set of M_{tx} transmit directions—or a *transmit coverage region*—that our codebook aims to transmit toward, and let $\mathcal{A}_{\mathrm{tx}}$ be a set of M_{rx} receive directions—or a *receive coverage region*—that our codebook aims to receive from.

$$\mathcal{A}_{\mathrm{tx}} = \left\{ \vartheta_{\mathrm{tx}}^{(i)} : i = 1, \ldots, M_{\mathrm{tx}} \right\} \quad (2)$$

$$\mathcal{A}_{\mathrm{rx}} = \left\{ \vartheta_{\mathrm{rx}}^{(j)} : j = 1, \ldots, M_{\mathrm{rx}} \right\} \quad (3)$$

Let $\mathbf{A}_{\mathrm{tx}} \in \mathbb{C}^{N_{\mathrm{t}} \times M_{\mathrm{tx}}}$ be the matrix of transmit array response vectors evaluated at the directions in $\mathcal{A}_{\mathrm{tx}}$, and let $\mathbf{A}_{\mathrm{rx}} \in \mathbb{C}^{N_{\mathrm{r}} \times M_{\mathrm{rx}}}$ be the matrix of receive array response vectors evaluated at the directions in $\mathcal{A}_{\mathrm{rx}}$.

$$\mathbf{A}_{\mathrm{tx}} = \left[\mathbf{a}_{\mathrm{tx}}\left(\vartheta_{\mathrm{tx}}^{(1)}\right) \quad \mathbf{a}_{\mathrm{tx}}\left(\vartheta_{\mathrm{tx}}^{(2)}\right) \quad \cdots \quad \mathbf{a}_{\mathrm{tx}}\left(\vartheta_{\mathrm{tx}}^{(M_{\mathrm{tx}})}\right)\right] \tag{4}$$

$$\mathbf{A}_{\mathrm{rx}} = \left[\mathbf{a}_{\mathrm{rx}}\left(\vartheta_{\mathrm{rx}}^{(1)}\right) \quad \mathbf{a}_{\mathrm{rx}}\left(\vartheta_{\mathrm{rx}}^{(2)}\right) \quad \cdots \quad \mathbf{a}_{\mathrm{rx}}\left(\vartheta_{\mathrm{rx}}^{(M_{\mathrm{rx}})}\right)\right] \tag{5}$$

We index the M_{tx} beams in $\bar{\mathcal{F}}$ and the M_{rx} beams in $\bar{\mathcal{W}}$ according to $\mathcal{A}_{\mathrm{tx}}$ and $\mathcal{A}_{\mathrm{rx}}$, respectively, as $\bar{\mathcal{F}} = \{\mathbf{f}_1, \ldots, \mathbf{f}_{M_{\mathrm{tx}}}\}$ and $\bar{\mathcal{W}} = \{\mathbf{w}_1, \ldots, \mathbf{w}_{M_{\mathrm{rx}}}\}$, where $\mathbf{f}_i \in \mathcal{F}$ is responsible for transmitting toward $\vartheta_{\mathrm{tx}}^{(i)}$ and $\mathbf{w}_j \in \mathcal{W}$ is responsible for receiving from $\vartheta_{\mathrm{rx}}^{(j)}$. Using this notation, we build the codebook matrix $\mathbf{F}$ by stacking transmit beams $\mathbf{f}_i$ as follows and the codebook matrix $\mathbf{W}$ analogously.

$$\mathbf{F} = \left[\mathbf{f}_1 \quad \mathbf{f}_2 \quad \cdots \quad \mathbf{f}_{M_{\mathrm{tx}}}\right] \in \mathbb{C}^{N_{\mathrm{t}} \times M_{\mathrm{tx}}} \tag{6}$$

$$\mathbf{W} = \left[\mathbf{w}_1 \quad \mathbf{w}_2 \quad \cdots \quad \mathbf{w}_{M_{\mathrm{rx}}}\right] \in \mathbb{C}^{N_{\mathrm{r}} \times M_{\mathrm{rx}}} \tag{7}$$

The coupling between the i-th transmit beam $\mathbf{f}_i$ and the j-th receive beam $\mathbf{w}_j$ can be captured by the product $\mathbf{w}_j^* \mathbf{H} \mathbf{f}_i$, which can be extended to all beam pairs as $\mathbf{W}^* \mathbf{H} \mathbf{F} \in \mathbb{C}^{M_{\mathrm{rx}} \times M_{\mathrm{tx}}}$. Our design aims to minimize the *average* coupling between beam pairs, which we denote E and write as

$$E = \frac{1}{M_{\mathrm{tx}} M_{\mathrm{rx}}} \cdot \left\| \mathbf{W}^* \mathbf{H} \mathbf{F} \right\|_{\mathrm{F}}^2. \tag{8}$$

In our design's attempt to minimize E, we must also ensure that the beams in $\mathbf{F}$ and $\mathbf{W}$ remain useful in serving users within the coverage region; of course, unconstrained, $\mathbf{F}$ and $\mathbf{W}$ minimize E when driven to $\mathbf{0}$. Notice that our definition of E neglects the large-scale channel gain G and transmit gain P, which would merely scale E. We now quantify a means to constrain our design to ensure it can maintain service.

Let $G_{\mathrm{tx,max}}^2 = N_{\mathrm{t}}^2$ and $G_{\mathrm{rx,max}}^2 = N_{\mathrm{r}}^2$ be the maximum transmit and receive power gain possible by our arrays, which can be achieved toward ϑ with $\mathbf{f} = \mathbf{a}_{\mathrm{tx}}(\vartheta)$ and $\mathbf{w} = \mathbf{a}_{\mathrm{rx}}(\vartheta)$, respectively. Let $G_{\mathrm{tx}}^2\left(\vartheta_{\mathrm{tx}}^{(i)}\right)$ be the transmit power gain afforded by $\mathbf{f}_i$ in the direction of $\vartheta_{\mathrm{tx}}^{(i)}$ and $G_{\mathrm{rx}}^2\left(\vartheta_{\mathrm{rx}}^{(j)}\right)$ be the receive power gain afforded by $\mathbf{w}_j$ in the direction of $\vartheta_{\mathrm{rx}}^{(j)}$, which can be written as

$$G_{\mathrm{tx}}^2\left(\vartheta_{\mathrm{tx}}^{(i)}\right) = \left| \mathbf{a}_{\mathrm{tx}}\left(\vartheta_{\mathrm{tx}}^{(i)}\right)^* \mathbf{f}_i \right|^2 \leq G_{\mathrm{tx,max}}^2 \tag{9}$$

$$G_{\mathrm{rx}}^2\left(\vartheta_{\mathrm{rx}}^{(j)}\right) = \left| \mathbf{a}_{\mathrm{rx}}\left(\vartheta_{\mathrm{rx}}^{(j)}\right)^* \mathbf{w}_j \right|^2 \leq G_{\mathrm{rx,max}}^2 \tag{10}$$

To offer our design flexibility in reducing E, we tolerate some loss in beamforming gain toward our desired directions; in other words, we will aim for some beamforming gain less than $G_{\mathrm{tx,max}}^2$ and $G_{\mathrm{rx,max}}^2$ in exchange for improved self-interference rejection. Let $G_{\mathrm{tx,tgt}}^2$ and $G_{\mathrm{rx,tgt}}^2$ be the following *target* transmit and receive beamforming gains for any transmit beam $\mathbf{f}_i$ or receive beam $\mathbf{w}_j$, respectively, in the direction it intends to serve.

$$G_{\mathrm{tx,tgt}}^2 = \Delta_{\mathrm{tx}}^2 \cdot G_{\mathrm{tx,max}}^2 \tag{11}$$

$$G_{\mathrm{rx,tgt}}^2 = \Delta_{\mathrm{rx}}^2 \cdot G_{\mathrm{rx,max}}^2 \tag{12}$$

Here, $0 < \Delta_{\mathrm{tx}}^2 \leq 1$ and $0 < \Delta_{\mathrm{rx}}^2 \leq 1$ are tolerated losses in beamforming gain (design parameters) that can be chosen by system engineers. Note that specific target gains for each beam in each codebook can be defined uniquely, though we use a common target codebook-wide for simplicity.

To quantify each transmit and receive beam approximately meeting the target gains in (11) and (12), we introduce a variance tolerance for each. Let $\sigma_{\mathrm{tx}}^2 \geq 0$ be the maximum variance tolerated in achieving the target transmit (magnitude) gain $G_{\mathrm{tx,tgt}}$ across beams in the transmit codebook $\bar{\mathcal{F}}$, normalized to $G_{\mathrm{tx,tgt}}^2$. Defining $\sigma_{\mathrm{rx}}^2 \geq 0$ analogously, we have

$$\frac{1}{M_{\mathrm{tx}}} \cdot \sum_{i=1}^{M_{\mathrm{tx}}} \frac{\left| G_{\mathrm{tx,tgt}} - G_{\mathrm{tx}}\left(\vartheta_{\mathrm{tx}}^{(i)}\right) \right|^2}{G_{\mathrm{tx,tgt}}^2} \leq \sigma_{\mathrm{tx}}^2 \tag{13}$$

$$\frac{1}{M_{\mathrm{rx}}} \cdot \sum_{j=1}^{M_{\mathrm{rx}}} \frac{\left| G_{\mathrm{rx,tgt}} - G_{\mathrm{rx}}\left(\vartheta_{\mathrm{rx}}^{(j)}\right) \right|^2}{G_{\mathrm{rx,tgt}}^2} \leq \sigma_{\mathrm{rx}}^2. \tag{14}$$

B. Assembling our Codebook Design Problem

With expressions for our codebook design criteria in hand, we now turn our attention to assembling a formal design problem. Let $\mathbf{g}_{\mathrm{tx}}^{\mathrm{tgt}} = G_{\mathrm{tx,tgt}} \cdot \mathbf{1}_{M_{\mathrm{tx}}}$ and $\mathbf{g}_{\mathrm{rx}}^{\mathrm{tgt}} = G_{\mathrm{rx,tgt}} \cdot \mathbf{1}_{M_{\mathrm{rx}}}$ be vectors containing the target transmit and receive gains at each entry. Using this, the expressions of (13) and (14) can be written equivalently (up to an arbitrary phase shift of $\mathbf{f}_i$ or $\mathbf{w}_j$) as follows, which we refer to as our *coverage constraints*,

$$\left\| \mathbf{g}_{\mathrm{tx}}^{\mathrm{tgt}} - \mathrm{diag}\left(\mathbf{A}_{\mathrm{tx}}^* \mathbf{F}\right) \right\|_2^2 \leq \sigma_{\mathrm{tx}}^2 \cdot G_{\mathrm{tx,tgt}}^2 \cdot M_{\mathrm{tx}} \tag{15}$$

$$\left\| \mathbf{g}_{\mathrm{rx}}^{\mathrm{tgt}} - \mathrm{diag}\left(\mathbf{A}_{\mathrm{rx}}^* \mathbf{W}\right) \right\|_2^2 \leq \sigma_{\mathrm{rx}}^2 \cdot G_{\mathrm{rx,tgt}}^2 \cdot M_{\mathrm{rx}} \tag{16}$$

where the (i,i)-th entry of $\mathbf{A}_{\mathrm{tx}}^* \mathbf{F}$ has magnitude $G_{\mathrm{tx}}\left(\vartheta_{\mathrm{tx}}^{(i)}\right)$ and the (j,j)-th entry of $\mathbf{A}_{\mathrm{rx}}^* \mathbf{W}$ has magnitude $G_{\mathrm{rx}}\left(\vartheta_{\mathrm{rx}}^{(j)}\right)$. By satisfying (15) and (16), we can ensure that our codebooks $\bar{\mathcal{F}}$ and $\bar{\mathcal{W}}$ adequately serve our coverage regions.

Using these coverage constraints, we formulate the following design problem to reduce E while maintaining coverage and satisfying quantized phase and amplitude control.

$$\min_{\mathbf{F}, \mathbf{W}} \ \left\| \mathbf{W}^* \mathbf{H} \mathbf{F} \right\|_{\mathrm{F}}^2 \tag{17a}$$

$$\text{s.t.} \ \left\| \mathbf{g}_{\mathrm{tx}}^{\mathrm{tgt}} - \mathrm{diag}\left(\mathbf{A}_{\mathrm{tx}}^* \mathbf{F}\right) \right\|_2^2 \leq \sigma_{\mathrm{tx}}^2 \cdot G_{\mathrm{tx,tgt}}^2 \cdot M_{\mathrm{tx}} \tag{17b}$$

$$\left\| \mathbf{g}_{\mathrm{rx}}^{\mathrm{tgt}} - \mathrm{diag}\left(\mathbf{A}_{\mathrm{rx}}^* \mathbf{W}\right) \right\|_2^2 \leq \sigma_{\mathrm{rx}}^2 \cdot G_{\mathrm{rx,tgt}}^2 \cdot M_{\mathrm{rx}} \tag{17c}$$

$$[\mathbf{F}]_{:,i} \in \mathcal{F} \ \forall \ i = 1, \ldots, M_{\mathrm{tx}} \tag{17d}$$

$$[\mathbf{W}]_{:,j} \in \mathcal{W} \ \forall \ j = 1, \ldots, M_{\mathrm{rx}} \tag{17e}$$

Decreasing $G_{\mathrm{tx,tgt}}^2$ and $G_{\mathrm{rx,tgt}}^2$ will relax the constraints of our design, allowing it to better reduce self-interference coupled by our transmit and receive beams; this helps facilitate full-duplexing service to two devices but degrades the service each device experiences. Increasing σ_{tx}^2 and σ_{rx}^2 will increase the flexibility of our design but weakens the coverage guarantee.

C. Solving our Codebook Design Problem

Having arrived at our design problem (17), we now set out to solve for our design. The non-convexity posed by digitally-controlled phase shifters and attenuators, captured by (17d) and (17e), presents difficulty in solving this problem. In general, we found that we cannot handle this non-convexity by merely ignoring it, solving, and then projecting the solutions $\mathbf{F}^\star$ and $\mathbf{W}^\star$ onto $\mathcal{F}$ and $\mathcal{W}$, respectively, though this may offer reasonable results when b_{phs} and b_{amp} are sufficiently high. To present a general approach to handling this non-convexity, we present the following alternating minimization with the understanding that more sophisticated algorithms can only improve the results we observe.

We define $\Pi_{\mathcal{A}}(\mathbf{A})$ as the projection of the elements of $\mathbf{A}$ onto the set $\mathcal{A}$. Our algorithm begins by initializing $\mathbf{F}$ and $\mathbf{W}$ as the projections of scaled $\mathbf{A}_{\mathrm{tx}}$ and $\mathbf{A}_{\mathrm{rx}}$ onto $\mathcal{F}$ and $\mathcal{W}$, respectively, quantizing their entries to have phase and amplitude resolutions b_{phs} and b_{amp}. That is, $\mathbf{F} \leftarrow \Pi_{\mathcal{F}}(\mathbf{A}_{\mathrm{tx}} \cdot \Delta_{\mathrm{tx}})$ and $\mathbf{W} \leftarrow \Pi_{\mathcal{W}}(\mathbf{A}_{\mathrm{rx}} \cdot \Delta_{\mathrm{rx}})$, which initializes our beams to achieve gains $G^2_{\mathrm{tx,tgt}}$ and $G^2_{\mathrm{rx,tgt}}$ across $\mathcal{A}_{\mathrm{tx}}$ and $\mathcal{A}_{\mathrm{rx}}$, respectively.

In this approach, we approximately solve problem (17) by solving for the codebooks beam-by-beam. We separate problem (17) into problems (18) and (20) below, which solve for the i-th transmit beam and j-th receive beam, respectively. Problems (18) and (20) are convex since they remove the hardware constraints and can be readily solved using a convex solver (we used [15]). We solve for the i-th transmit beam $\mathbf{f}_i$ in problem (18), starting with $i = 1$ and the initialized $\mathbf{W}$.

$$\min_{\mathbf{f}_i} \ \left\| \mathbf{W}^* \mathbf{H} \mathbf{f}_i \right\|_2 \tag{18a}$$

$$\text{s.t.} \ \left| G_{\mathrm{tx,tgt}} - \mathbf{a}_{\mathrm{tx}}\left(\vartheta_{\mathrm{tx}}^{(i)}\right)^* \mathbf{f}_i \right|^2 \leq \sigma_{\mathrm{tx}}^2 \cdot G_{\mathrm{tx,tgt}}^2 \tag{18b}$$

$$\left| [\mathbf{f}_i]_n \right| \leq 1 \ \forall \ n = 1, \ldots, N_{\mathrm{t}} \tag{18c}$$

Then, the solution $\mathbf{f}_i^\star$ is projected onto the set $\mathcal{F}$ before updating it in the matrix $\mathbf{F}$.

$$[\mathbf{F}]_{:,i} \leftarrow \Pi_{\mathcal{F}}\left(\mathbf{f}_i^\star\right) \tag{19}$$

The updated $\mathbf{F}$ is then used when solving for the j-th receive beam (beginning with $j = 1$) in problem (20).

$$\min_{\mathbf{w}_j} \ \left\| \mathbf{w}_j^* \mathbf{H} \mathbf{F} \right\|_2 \tag{20a}$$

$$\text{s.t.} \ \left| G_{\mathrm{rx,tgt}} - \mathbf{a}_{\mathrm{rx}}\left(\vartheta_{\mathrm{rx}}^{(j)}\right)^* \mathbf{w}_j \right|^2 \leq \sigma_{\mathrm{rx}}^2 \cdot G_{\mathrm{rx,tgt}}^2 \tag{20b}$$

$$\left| [\mathbf{w}_j]_n \right| \leq 1 \ \forall \ = 1, \ldots, N_{\mathrm{r}} \tag{20c}$$

The solution $\mathbf{w}_j^\star$ is then projected onto $\mathcal{W}$ before updating $\mathbf{W}$.

$$[\mathbf{W}]_{:,j} \leftarrow \Pi_{\mathcal{W}}\left(\mathbf{w}_j^\star\right) \tag{21}$$

We iteratively solve for the $(i+1)$-th transmit beam and then the $(j+1)$-th receive beam until all M_{tx} and M_{rx} beams are solved for. When $M_{\mathrm{tx}} \neq M_{\mathrm{rx}}$, the remaining transmit/receive beams can be solved for after $\min(M_{\mathrm{tx}}, M_{\mathrm{rx}})$ iterations. We have found that this iterative approach handles the quantization of $\mathbf{F}$ and $\mathbf{W}$ quite well by *progressively* incorporating quantization beam-by-beam, allowing later beams to account for the quantization imposed on earlier beams.

IV. Numerical Results

To evaluate our design, we simulated a simple 30 GHz network where a full-duplex transceiver transmits to a downlink user and receives from an uplink user. The two users are equipped with a single antenna while the full-duplex device has two 8×8 half-wavelength uniform planar arrays (UPAs) one for transmission and one for reception. We drew realizations of our network in a Monte Carlo fashion. The channel vectors $\mathbf{h}_{\mathrm{tx}} \in \mathbb{C}^{64\times 1}$ to the downlink user and $\mathbf{h}_{\mathrm{rx}} \in \mathbb{C}^{64\times 1}$ to the uplink user are simulated as line-of-sight (LOS) channels with normally distributed gain, where users are distributed uniformly across the transmit/receive coverage regions at each realization. For the self-interference channel $\mathbf{H}$, we consider the spherical-wave channel model [16], which captures idealized near-field interaction between the transmit and receive arrays of the full-duplex device, described as

$$[\mathbf{H}]_{m,n} = \frac{\gamma}{r_{n,m}} \exp\left(-\mathrm{j}2\pi \frac{r_{n,m}}{\lambda}\right) \tag{22}$$

where $r_{n,m}$ is the distance between the n-th transmit antenna and the m-th receive antenna, λ is the carrier wavelength, and γ is a normalizing factor to satisfy $\|\mathbf{H}\|_{\mathrm{F}}^2 = N_{\mathrm{t}} N_{\mathrm{r}}$. To realize such a channel, we have separated our transmit and receive arrays by 10λ in the azimuth plane. While this model may not hold in practice, it provides us a sensible starting point to evaluate our design when the self-interference channel is dominated by near-field interaction.

Our transmit and receive coverage regions are comprised of uniformly spaced points in azimuth from $-60°$ to $60°$ with $15°$ spacing and in elevation from $-30°$ to $30°$ with $15°$ spacing. This amounts to $M_{\mathrm{tx}} = M_{\mathrm{rx}} = 45$ total directions in $\mathcal{A}_{\mathrm{tx}}$ and $\mathcal{A}_{\mathrm{rx}}$. We have assumed the analog beamforming networks use log-stepped attenuators with 0.25 dB of attenuation per LSB.

We assess our design with sum spectral efficiency of the transmit and receive links. Suppose the transmit and receive links have signal-to-noise ratios (SNRs) $\mathrm{SNR}_{\mathrm{tx}}$ and $\mathrm{SNR}_{\mathrm{rx}}$, respectively, which capture the received powers relative to noise *without* beamforming. Transmitting with beamformer $\mathbf{f}$, the downlink user can achieve a spectral efficiency

$$R_{\mathrm{tx}} = \log_2\left(1 + \frac{\mathrm{SNR}_{\mathrm{tx}}}{N_{\mathrm{t}}} \cdot \left|\mathbf{h}_{\mathrm{tx}}^* \mathbf{f}\right|^2\right) \tag{23}$$

where N_{t}^{-1} handles power splitting in the transmit beamforming network. Plagued by self-interference, the uplink user sees

$$R_{\mathrm{rx}} = \log_2\left(1 + \frac{\mathrm{SNR}_{\mathrm{rx}} \cdot \left|\mathbf{w}^* \mathbf{h}_{\mathrm{rx}}\right|^2}{\|\mathbf{w}\|_2^2 + \mathrm{INR} \cdot \left|\mathbf{w}^* \mathbf{H} \mathbf{f}\right|^2}\right) \tag{24}$$

where $\left|\mathbf{w}^* \mathbf{H} \mathbf{f}\right|^2$ is the self-interference coupling factor between the transmit and receive beams and $\mathrm{INR} = P \cdot G^2 / N_0$ is the interference-to-noise ratio (INR) of self-interference without beamforming; N_0 is the additive noise variance. INR is an important quantity for evaluating this work since it captures the *isolation* G^{-2} between the transmit and receive arrays, allowing us to abstract it from the *spatial* coupling of transmit and receive beams. The INR of a mmWave

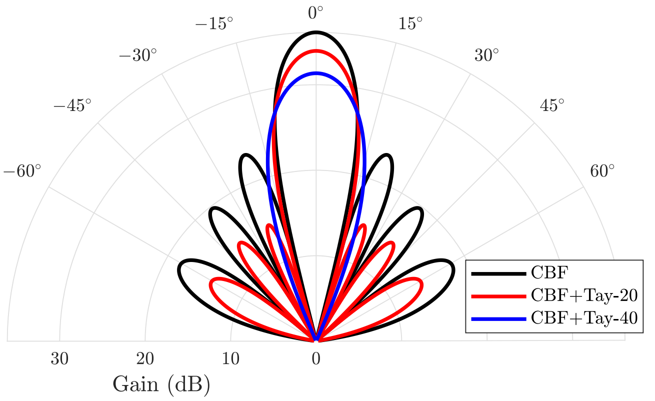

Fig. 2. The azimuth cut of a broadside beam from each benchmark codebook.

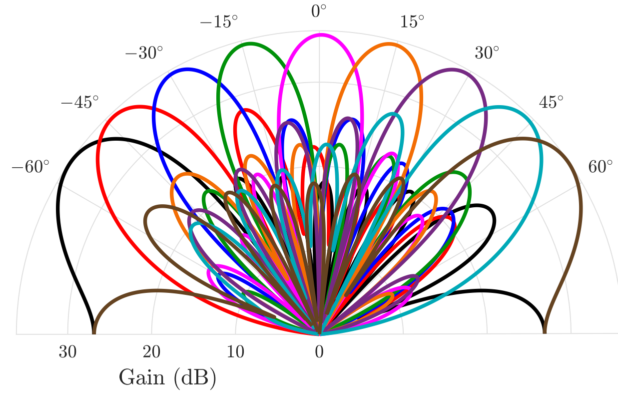

Fig. 3. The azimuth cuts of beams from our transmit codebook serving various azimuth directions at an elevation of $0°$.

full-duplex system depends on a variety of factors including transmit power, noise power, and system setup. The uplink and downlink spectral efficiencies are bounded by their Shannon capacities (neglecting self-interference on the uplink) with unconstrained beams $\mathbf{f}$ and $\mathbf{w}$. The sum spectral efficiency $R_{\mathrm{tx}} + R_{\mathrm{rx}}$ is bounded by the full-duplex capacity C_{fd}, the sum of the two Shannon capacities. Under equal time-division duplexing (TDD), the half-duplex capacity is simply $C_{\mathrm{hd}} = 0.5 \cdot C_{\mathrm{fd}}$. Note that the use of beamforming codebooks will naturally fall short of these capacities.

Considering ours is the first known codebook design *for mmWave full-duplex*, we evaluate our codebook design against the following three conventional codebooks: (i) conjugate beamforming (CBF) where $\mathbf{f}_i = \mathbf{a}_{\mathrm{tx}}\left(\vartheta_{\mathrm{tx}}^{(i)}\right)$ and $\mathbf{w}_j = \mathbf{a}_{\mathrm{rx}}\left(\vartheta_{\mathrm{rx}}^{(j)}\right)$; (ii) CBF+Tay-20 where $\mathbf{f}_i = \mathbf{a}_{\mathrm{tx}}\left(\vartheta_{\mathrm{tx}}^{(i)}\right) \odot \mathbf{v}$ and $\mathbf{w}_j = \mathbf{a}_{\mathrm{rx}}\left(\vartheta_{\mathrm{rx}}^{(j)}\right) \odot \mathbf{v}$ and $\mathbf{v}$ is a Taylor window with 20 dB of side lobe suppression applied element-wise; and (iii) CBF+Tay-40, defined as in CBF+Tay-20, except $\mathbf{v}$ is a Taylor window with 40 dB of side lobe suppression. The beam pattern of each of our three codebooks is shown in Fig. 2. CBF offers maximum beamforming gain with a narrow main lobe but exhibits high side lobe levels. Taylor windowing reduces the side lobe levels at the cost of lessened beamforming gain and a wider main lobe (e.g., CBF+Tay-20 and CBF+Tay-40 lose about 2 dB and 5 dB in beamforming gain, respectively).

Let us begin by visually inspecting the beams produced by our codebook design, which we illustrate in Fig. 3. We designed our codebooks using $\Delta_{\mathrm{tx}}^2 = \Delta_{\mathrm{rx}}^2 = 0$ dB and $\sigma_{\mathrm{tx}}^2 = \sigma_{\mathrm{rx}}^2 = -20$ dB, where we expect our beams to have nearly full transmit/receive gain and some flexibility in meeting this gain. We use phase and attenuator resolutions $b_{\mathrm{phs}} = b_{\mathrm{amp}} = 5$ bits, which can be found in commercial phased arrays. First, we note that our beams cover $-60°$ to $60°$ in $15°$ steps as was specified by our transmit and receive coverage regions. A user falling anywhere in the transmit/receive coverage region can confidently expect to see high gain. Notice that our design appears to creatively shape side lobes, rather than merely shrinking them; this is its attempt to strategically cancel self-interference *spatially*.

Now, in Fig. 4, we evaluate the sum spectral efficiency $R_{\mathrm{tx}} + R_{\mathrm{rx}}$ offered by the considered benchmarks versus our codebook for various resolutions $b_{\mathrm{phs}} = b_{\mathrm{amp}} \in \{5, 6, 7, 8\}$ bits. We begin by fixing $\mathrm{SNR}_{\mathrm{tx}} = \mathrm{SNR}_{\mathrm{rx}} = 0$ dB and varying INR from -30 dB to 130 dB. At $\mathrm{INR} \ll 0$ dB, the inherent isolation between the transmit and receive arrays is high, meaning the system can operate in full-duplex fashion, even with high coupling between transmit and receive beams. This is clearly seen for all codebooks shown in Fig. 4, where they all maintain appreciable fractions of the full-duplex capacity at low INR. CBF beams offer maximal beamforming gain and thus the highest sum spectral efficiency at low INR, with our design just below. The other two benchmarks fall below due to their tradeoff of beamforming gain for side lobe suppression.

As INR increases, the coupling between transmit and receive beams plays a significant role in what level of self-interference is present, and thus, what uplink spectral efficiency R_{rx} is achieved. Notice that the CBF codebook begins to taper off first as INR is increased, followed by CBF+Tay-20 and CBF+Tay-40 courtesy of their side lobe suppression. Our design, on the other hand, is comparable or outperforms all three benchmarks across all INR thanks to its robustness to self-interference. From $\mathrm{INR} = 10$ dB to $\mathrm{INR} = 80$ dB or more, our design outperforms all three conventional codebooks. At a sum spectral efficiency of 8 bps/Hz, we can see that our design offers 20 dB of robustness to INR with $b_{\mathrm{phs}} = b_{\mathrm{amp}} = 5$ bits versus the conventional codebooks; with each added bit, we gain approximately 10 dB of robustness. When $\mathrm{INR} \to 130$ dB, the system becomes overwhelmed with self-interference driving $R_{\mathrm{rx}} \to 0$ bps/Hz, even with our design's low coupling between transmit and receive beams.

Now, we consider Fig. 5, where we fix $\mathrm{INR} = 60$ dB, vary $\mathrm{SNR}_{\mathrm{tx}} = \mathrm{SNR}_{\mathrm{rx}}$, and use the same design parameters as before. At low $\mathrm{SNR}_{\mathrm{tx}} = \mathrm{SNR}_{\mathrm{rx}}$, we notice that CBF offers higher sum spectral efficiency than CBF+Tay-40, thanks to its higher beamforming gain, which is more important at low SNR than interference suppression. As $\mathrm{SNR}_{\mathrm{tx}} = \mathrm{SNR}_{\mathrm{rx}}$ increases, the interference mitigation offered by CBF+Tay-40 nets it a higher sum spectral efficiency over CBF. Our design,

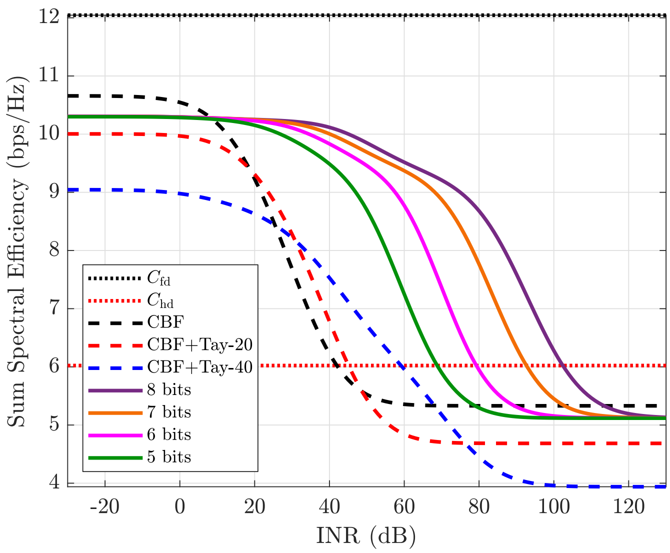

Fig. 4. Sum spectral efficiency $R_{\text{tx}} + R_{\text{rx}}$ as a function of INR for various codebooks, where $\text{SNR}_{\text{tx}} = \text{SNR}_{\text{rx}} = 0$ dB.

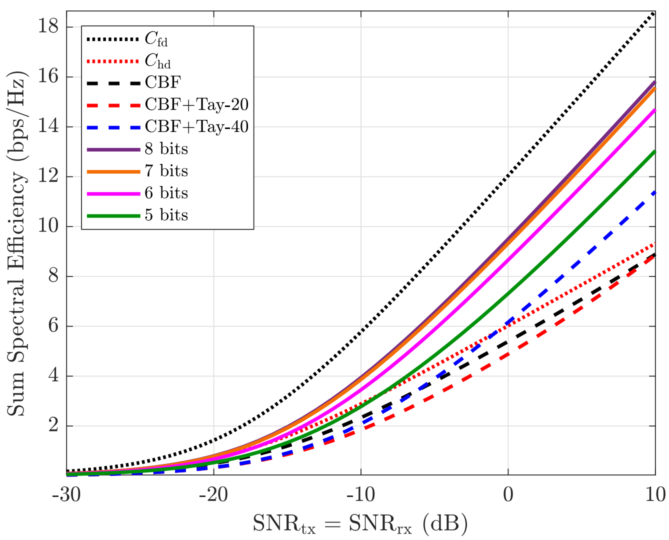

Fig. 5. Sum spectral efficiency $R_{\text{tx}} + R_{\text{rx}}$ as a function of $\text{SNR}_{\text{tx}} = \text{SNR}_{\text{rx}}$ for various codebooks, where $\text{INR} = 60$ dB.

shown for various $b_{\text{phs}} = b_{\text{amp}}$, outperforms all designs across $\text{SNR}_{\text{tx}} = \text{SNR}_{\text{rx}}$ thanks to its robustness to self-interference even at this high INR. Notice that our design, along with CBF+Tay-40, reaches a high-SNR (approximately linear) regime much sooner than CBF and CBF+Tay-20 due to better self-interference rejection. With higher $b_{\text{phs}} = b_{\text{amp}}$, as highlighted before, our design can achieve significant jumps in sum spectral efficiency, albeit with diminishing returns.

V. Conclusion

To our knowledge, we have presented the first design of analog beamforming codebooks for mmWave full-duplex, where we construct sets of transmit and receive beams that offer high beamforming gain while simultaneously reducing the amount of self-interference coupled between transmit-receive beam pairs. Numerical results show that our design outperforms off-the-shelf codebooks and confirms that full-duplex mmWave systems can benefit from dedicated codebook designs offering robustness to self-interference without comprising beamforming gain. With our codebooks, full-duplex mmWave systems can support codebook-based beam alignment while also minimizing self-interference. Our codebooks have the potential to improve a variety of existing mmWave full-duplex solutions and can be supplemented by analog and digital self-interference cancellation. Important future work includes characterizing the self-interference channel and designing codebooks robust to imperfect channel knowledge.

Acknowledgments

I. P. Roberts is supported by the National Science Foundation under Grant No. DGE-1610403. Any opinions, findings, and conclusions or recommendations expressed in this material are those of the authors and do not necessarily reflect the views of the National Science Foundation.

References

[1] R. W. Heath *et al.*, "An overview of signal processing techniques for millimeter wave MIMO systems," *IEEE J. Sel. Topics Signal Process.*, vol. 10, no. 3, pp. 436–453, Apr. 2016.

[2] J. Wang *et al.*, "Beam codebook based beamforming protocol for multi-Gbps millimeter-wave WPAN systems," *IEEE JSAC*, vol. 27, no. 8, pp. 1390–1399, Oct. 2009.

[3] R. W. Heath Jr. and A. Lozano, *Foundations of MIMO Communication*. Cambridge University Press, 2018.

[4] I. P. Roberts, J. G. Andrews, H. B. Jain, and S. Vishwanath, "Millimeter-wave full duplex radios: New challenges and techniques," *IEEE Wireless Commun.*, pp. 36–43, Feb. 2021.

[5] K. Satyanarayana *et al.*, "Hybrid beamforming design for full-duplex millimeter wave communication," *IEEE Trans. Veh. Technol.*, vol. 68, no. 2, pp. 1394–1404, Feb. 2019.

[6] X. Liu *et al.*, "Beamforming based full-duplex for millimeter-wave communication," *Sensors*, vol. 16, no. 7, p. 1130, Jul. 2016.

[7] R. López-Valcarce and N. González-Prelcic, "Analog beamforming for full-duplex millimeter wave communication," in *Proc. Intl. Symp. Wireless Commun. Syst.*, Aug. 2019, pp. 687–691.

[8] ——, "Beamformer design for full-duplex amplify-and-forward millimeter wave relays," in *Proc. Intl. Symp. Wireless Commun. Syst.*, Aug. 2019, pp. 86–90.

[9] J. Palacios, J. Rodríguez-Fernández, and N. González-Prelcic, "Hybrid precoding and combining for full-duplex millimeter wave communication," in *Proc. IEEE Global Commun. Conf.*, Dec. 2019, pp. 1–6.

[10] L. Zhu *et al.*, "Millimeter-wave full-duplex UAV relay: Joint positioning, beamforming, and power control," *IEEE JSAC*, vol. 38, no. 9, pp. 2057–2073, Sep. 2020.

[11] Y. Cai *et al.*, "Robust joint hybrid transceiver design for millimeter wave full-duplex MIMO relay systems," *IEEE Trans. Wireless Commun.*, vol. 18, no. 2, pp. 1199–1215, Feb. 2019.

[12] I. P. Roberts and S. Vishwanath, "Beamforming cancellation design for millimeter-wave full-duplex," in *Proc. IEEE Global Commun. Conf.*, Dec. 2019, pp. 1–6.

[13] I. P. Roberts, H. B. Jain, and S. Vishwanath, "Equipping millimeter-wave full-duplex with analog self-interference cancellation," in *Proc. IEEE Intl. Conf. Commun. Wkshp.*, Jun. 2020.

[14] I. P. Roberts, J. G. Andrews, and S. Vishwanath, "Hybrid beamforming for millimeter wave full-duplex under limited receive dynamic range," *IEEE Trans. Wireless Commun.*, 2021, (to appear).

[15] M. Grant and S. Boyd, "CVX: Software for disciplined convex programming, version 2.1," http://cvxr.com/cvx, Mar. 2014.

[16] J.-S. Jiang and M. A. Ingram, "Spherical-wave model for short-range MIMO," *IEEE Trans. Commun.*, vol. 53, no. 9, pp. 1534–1541, Sep. 2005.